

## Investigation into the Synergistic Effect of Nano-sized Materials on the Anti-corrosion Properties of a Waterborne Epoxy Coating

Xiaoqing Xiao<sup>1\*\*</sup>, Dongmei Wang<sup>1\*\*</sup>, Yongxin Li<sup>1,4,\*</sup>, Emily Jackson<sup>4</sup>, Yida Fang<sup>4</sup>, Yan Zhang<sup>4</sup>, Ning Xie<sup>4</sup>, Xianming Shi<sup>2,3,4,\*</sup>

<sup>1</sup> College of Chemistry and Materials Science, Anhui Normal University, Wuhu 241000, China

<sup>2</sup> Department of Civil & Environmental Engineering, P. O. Box 642910, Washington State University, Pullman, WA 99164-2910, USA

<sup>3</sup> School of Civil Engineering and Architecture, Wuhan Polytechnic University, Wuhan, 430023, China.

<sup>4</sup> Western Transportation Institute, Montana State University, Bozeman, MT 59717-2220, USA.

\* E-mail: [yongli@mail.ahnu.edu.cn](mailto:yongli@mail.ahnu.edu.cn); [xianming.shi@wsu.edu](mailto:xianming.shi@wsu.edu)

\*\* Co-first authors

Received: 29 March 2016 / Accepted: 13 May 2016 / Published: 4 June 2016

---

A kind of environmentally friendly waterborne epoxy coating incorporating several nano-sized materials, nano-Fe<sub>2</sub>O<sub>3</sub>, multi-wall carbon nanotubes (CNTs), polysiloxane-modified montmorillonite, and non-modified montmorillonite, were successfully synthesized on the surface of steel substrates through a room-temperature curing method. Thirty-two nanocomposite coatings were formulated by varying the dosage of these four nanomaterials and a commercial corrosion inhibitor and by following a statistical design of experiments. The morphologies of the nanomaterials and cured epoxy coating or nanocomposite coatings were examined by scanning electron microscopy (SEM). The effect of incorporating nanomaterials at different ratios on the thermal property, mechanical property and anti-corrosion properties of the epoxy coating was investigated by differential scanning calorimetry (DSC), microhardness test, potentiodynamic polarization and electrochemical impedance spectroscopy (EIS), respectively. The results show that adding the nanomaterials at special ratios can significantly improve the mechanical and anti-corrosion properties of the epoxy coating. In particular, the concurrent incorporation of small amounts of ZPA, nano-Fe<sub>2</sub>O<sub>3</sub> and CNTs into the waterborne epoxy coating led to outstanding corrosion resistance on steel. This study sheds light on the multifunctional role of nanomaterials in modifying the microstructure and chemistry of the cured epoxy coating and in improving the coating/steel interface.

---

**Keywords:** interfaces; electrochemical techniques; coatings; electron microscopy; corrosion; Hardness

## 1. INTRODUCTION

The outstanding adhesion and affinity to heterogeneous materials, chemical resistance, processability, and electrical insulation properties have rendered epoxy-based resins one of the main materials for anti-corrosion coating applications.[1-4] For instance, epoxy-coated rebar has been extensively used in reinforced concrete structures to mitigate the rebar corrosion induced by chlorides [5-10]. Epoxy coatings can be utilized for protecting steel and other metallic substrates from corrosion mainly through two functions. First, the coating can serve as a physical barrier to slow down the ingress of deleterious species such as water, oxygen, and chlorides. The ingress rate and availability of chloride ions and oxygen can greatly affect the risk of corrosion initiation and propagation for rebar in concrete [11, 12]. Second, the coating can be used as a reservoir for corrosion inhibitors and other additives to protect the metal surface from the attack by different species such as chloride ions.

Two inherent weaknesses in typical epoxy coatings are their susceptibility to damage by surface abrasion and wear [6] and their poor resistance to the initiation and propagation of cracks [8], particularly in the presence of water. Both of these have hindered their expanded use for anti-corrosion and other applications. For instance, the surface damage of epoxy-coated rebar can pose significant risk for localized corrosion of the rebar in concrete [13]. The defects within the epoxy coating matrix probably will be acted as pathways, which can accelerate the ingress of water, oxygen and other aggressive species onto the substrate of metals, and reduce its function as a barrier layer and resulting in localized corrosion. Fibers and microcapsules are among the innovative materials to use for improving the coatings' resistance to abrasion and cracking and endowing them with self-healing capability, respectively [14-17]. Moreover, epoxy coatings tend to experience shrinkage with large volume upon curing and can absorb water from surroundings due to their hydrophilic property [7, 9]. Traditionally, such risks have been mitigated by incorporating a second phase that is miscible with the epoxy, such as dispersing inorganic filler particles into the epoxy resin matrix [11-13, 16, 17].

In this context, it is hypothesized that admixing certain type and amount of nano-sized materials into the epoxy can mitigate the above-mentioned weaknesses of traditional epoxy coatings. This hypothesis has been validated by recent studies. In recent years, introduction of various nanomaterials into epoxy coatings have attracted a great deal of attention as such nano-modification led to improvement of the coatings' mechanical, thermal and anti-corrosion properties [14, 15, 18-25]. Recently, Tang et al. reported that the addition of 10 wt.% of halloysite nanotubes (a type of nanoclay different from montmorillonite) greatly enhanced the epoxy resin's fracture toughness. Moreover, the chemical treatment and processing method both significantly affected the microstructure and fracture properties of halloysite-epoxy composites [25]. Zabihi et al. reported that the incorporation of 10 wt.% of  $\text{Fe}_2\text{O}_3$  nanoparticles into an epoxy resin significantly altered the reaction kinetics of epoxy and improved its cross-linking density [26]. Xu et al. reported that the incorporation of 3-10 wt.% of organophilic montmorillonite into an epoxy resin significantly altered the reaction kinetics of epoxy and decreased its glass transition temperature [27]. Khanbabaei et al. reported that the addition of 1-7 wt.% of an organically modified montmorillonite into an epoxy resin could potentially change its failure mode from brittle to tough, and could improve its impact strength and other mechanical properties [28]. Similarly, Wang et al. reported the storage modulus, Young's modulus and fracture

toughness could be improved greatly with the addition of 1-3 wt.% of silane-modified nanoclay into an epoxy resin [29].

Well-dispersed nanomaterials can provide an environmentally benign approach, which will greatly enhance the integrity and durability of cured epoxy coatings [22-24], likely attributable to the interfacial interactions between nanomaterials and the coating strongly. Such strong interactions are derived from the nanometer size and large specific surface area of nanomaterials. In addition to improving barrier properties for corrosion protection, nano-modification of epoxy coatings can decrease the trend for the coating to blister or delaminate [30].

Our previous work [1] demonstrated that admixing 1 wt.% of nano-silica and 1 wt.% of nano-Fe<sub>2</sub>O<sub>3</sub> substantially increased the nano-scale Young's modulus and anti-corrosion properties of a solvent-based epoxy coating, respectively. In this work, we will test the hypothesis that the combined use of various types of nanomaterials can lead to synergy between them, which will allow simultaneous improvements in both mechanical and anti-corrosion properties of a waterborne epoxy coating. Currently, this is still a relatively uncharted territory. Recently, Wang et al. reported the synergistic effect of two nanomaterials, layered montmorillonite (Na-MMT) at 0.25 wt.% and mesoporous silica particles (MCM-41) at 0.25 wt.%, on enhancing the barrier properties and thus corrosion resistance of an epoxy coating [31]. In this work, we will investigate the possible synergistic effect of some nanomaterials, including two nanoclays, nano-Fe<sub>2</sub>O<sub>3</sub>, multi-wall carbon nanotubes, and a commercial corrosion inhibitor, via a statistical design of experiments. It is expected to shed more light on the research of the fundamental mechanisms through which nanomaterials contribute to a better epoxy matrix and a better coating/steel interface.

## 2. EXPERIMENTAL

### 2.1. Materials

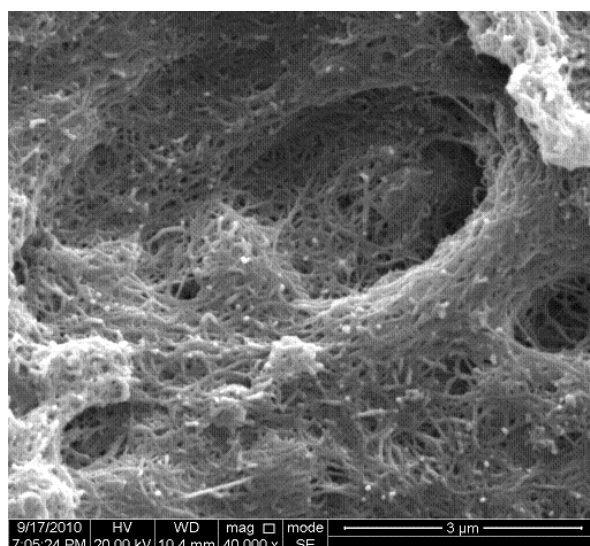
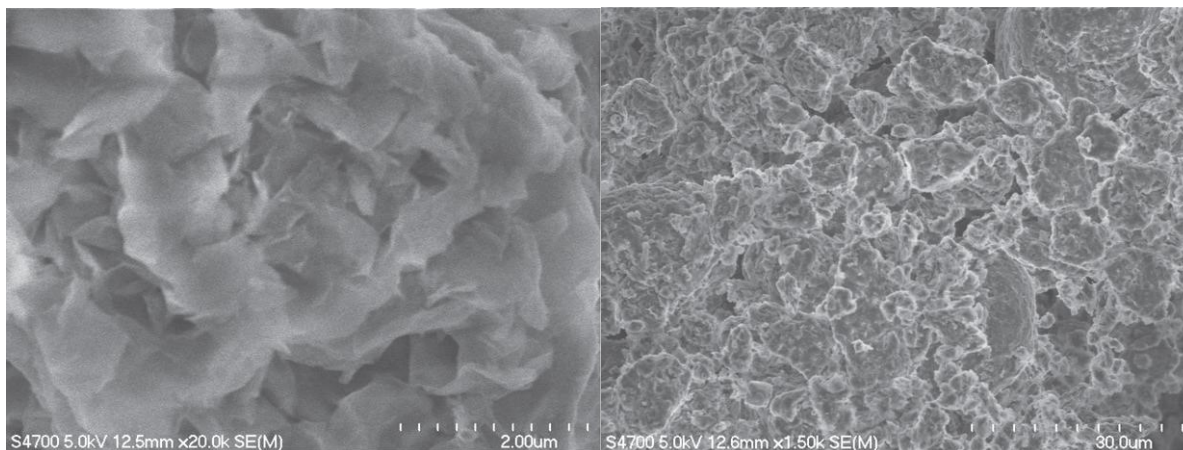
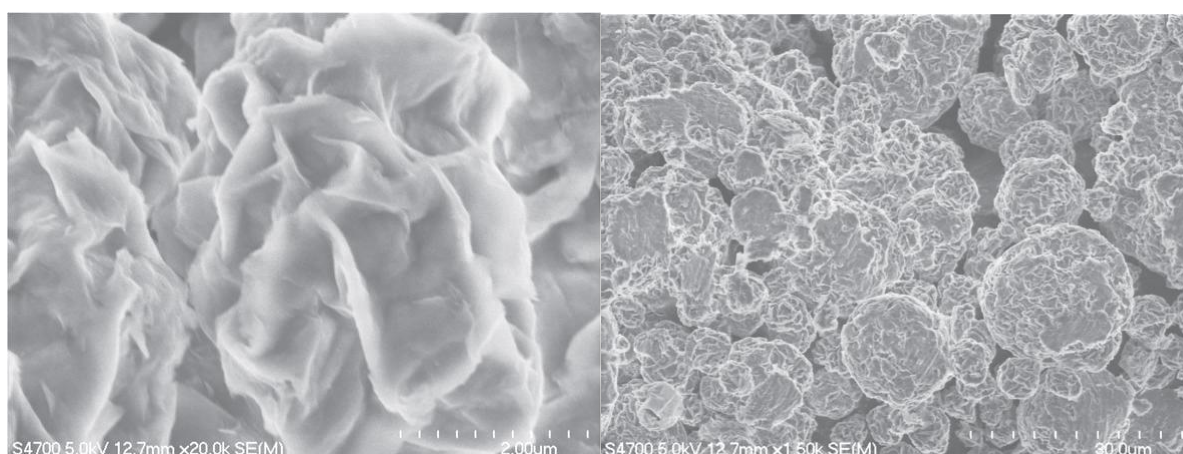


**Figure 1.** FE-SEM micrograph of MW-CNTs



(a)



(b)

**Figure 2.** FE-SEM micrographs of non-modified nanoclay (a) and polymer modified nanoclay (b) with different magnification (left: 20K; right: 150K)

The epoxy resin ANCAREX AR555 and its hardener ANQUAMINE 419 were purchased from Air Products and Chemicals, Inc. (Allentown, PA). Zinc - aluminum phosphate (ZPA) was an inorganic corrosion inhibitor obtained from Montana State University. Nano-Fe<sub>2</sub>O<sub>3</sub> was purchased from MTI Corporation (Richmond, CA). Polysiloxane-modified montmorillonite (PS-clay) and non-modified montmorillonite (Nano-clay) were purchased from Nanocor. Inc. (Hoffman Estates, IL). Multi-wall carbon nanotubes (CNTs), NC 7000, was obtained from Nanocyl<sup>TM</sup> (Belgium). The properties of nanomaterials can be found in our previous reports [32] and the morphologies of the nanomaterials are shown in Figure 1 and Figure 2. The steel coupons (surface area ~ 2 cm<sup>2</sup>) were purchased from Metal Samples (Munford, AL, USA), which were Cor-ten B type (UNS number K11430; density: 7.60 g/cm<sup>3</sup>; chemical composition: C 0.10–0.19%, Cr 0.40–0.65%, Cu 0.25–0.40%, Fe 97.0–98.2%, Mn 0.90–1.25%, P ≤ 0.04%, Si 0.15–0.30%, S ≤ 0.05%, V 0.02–0.10%).

## 2.2. Methods

### 2.2.1. Steel substrate preparation

The steel substrate preparation was similar to our previous work [21]. Briefly, a copper wire was electrically connected to the coupon's surface, and then all surfaces except the one exposed to electrolyte for corrosion testing were sealed with a thick bulk waterproof Marine Epoxy resin. After epoxy curing for ~ 2-3 days, the unsealed coupon surface was polished on silicon carbide (SiC) papers down to a grid size of 1000. Before test, the sample surface was rinsed with tap water, sonicated in de-ionized water and then rinsed with acetone.

### 2.2.2. Coating preparation:

**Table 1.** Thirty-two nanocomposite coatings formulated via uniform design (with various nanomaterials added by the total mass of the waterborne epoxy resin and its hardener, in %), vs. the plain epoxy coating as control (#33).

| RUNORD | ZPA | Nano-Fe <sub>2</sub> O <sub>3</sub> | PS-Clay | Nano-Clay | CNTs |
|--------|-----|-------------------------------------|---------|-----------|------|
| 1      | 1.5 | 0.7                                 | 0       | 0.15      | 0    |
| 2      | 1   | 0                                   | 1       | 0         | 0.1  |
| 3      | 0   | 0.4                                 | 1       | 0         | 0    |
| 4      | 1.5 | 0.7                                 | 0.5     | 0.75      | 0.1  |
| 5      | 1   | 0.7                                 | 1       | 0.75      | 0.02 |
| 6      | 0.5 | 0.4                                 | 0       | 0.75      | 0.02 |
| 7      | 0   | 0.7                                 | 0       | 0.45      | 0.02 |
| 8      | 0.5 | 0.7                                 | 1.5     | 0.45      | 0.1  |
| 9      | 1   | 0.4                                 | 1.5     | 0.15      | 0    |
| 10     | 1   | 1                                   | 0.5     | 0.15      | 0.02 |
| 11     | 0   | 0                                   | 0       | 0.15      | 0.1  |
| 12     | 1.5 | 0                                   | 1.5     | 0.45      | 0.05 |
| 13     | 0   | 0.4                                 | 1.5     | 0.75      | 0.1  |
| 14     | 1.5 | 0                                   | 0.5     | 0         | 0.02 |
| 15     | 0   | 0                                   | 0.5     | 0.45      | 0    |
| 16     | 1.5 | 1                                   | 1       | 0.15      | 0.1  |
| 17     | 0.5 | 0.7                                 | 0.5     | 0         | 0    |
| 18     | 1.5 | 1                                   | 1.5     | 0.75      | 0    |
| 19     | 0.5 | 1                                   | 1       | 0.45      | 0    |
| 20     | 1   | 0.4                                 | 0.5     | 0.45      | 0.1  |
| 21     | 0.5 | 0                                   | 1       | 0.75      | 0.05 |
| 22     | 1.5 | 0.4                                 | 1       | 0.45      | 0.02 |
| 23     | 0   | 1                                   | 1.5     | 0         | 0.02 |
| 24     | 1   | 0.7                                 | 1.5     | 0         | 0.05 |
| 25     | 0   | 1                                   | 0.5     | 0.75      | 0.05 |
| 26     | 0   | 0.7                                 | 1       | 0.15      | 0.05 |
| 27     | 1   | 1                                   | 0       | 0.45      | 0.05 |
| 28     | 0.5 | 1                                   | 0       | 0         | 0.1  |
| 29     | 1   | 0                                   | 0       | 0.75      | 0    |
| 30     | 0.5 | 0.4                                 | 0.5     | 0.15      | 0.05 |
| 31     | 0.5 | 0                                   | 1.5     | 0.15      | 0.02 |
| 32     | 1.5 | 0.4                                 | 0       | 0         | 0.05 |
| 33     | 0   | 0                                   | 0       | 0         | 0    |

Usually, the epoxy nanocomposites are fabricated through dispersing nanomaterials into the epoxy matrix either with a solvent or through a heating process. However, the latter process is always with poor dispersion due to the clustering or agglomeration of nanomaterials. The use of solvent can get the good dispersal of nanomaterials in the resin, but the solvent should be removed with vacuum evaporation and then the curing agents can be added to the mixture, which will lead to undermine the homogeneity of the nanocomposites after curing, especially when a high nanomaterials loading is used. To solve this issue, Sun et al. developed a method to add the curing agent to the mixture before removing the solvent, which can improve the dispersion of nanomaterials in the coating layer [33]. In addition, Sun et al. also find that the slurry can be directly applied on the surface of metallic substrates to form a uniform thin barrier coating [33]. In this work, both resin and its hardener were diluted separately by water at a 1:1 weight ratio before test. Nanomaterials, at various percentage (shown in Table 1) of the total weight of resin and hardener, were added to the resin-water solution, followed by stirring at speeds up to 1550 rpm (Model 14-503, Fisher Scientific, Inc.) and sonication (Model 50 T, VWR, West Chester, PA, USA) for 10 min.

After that, the hardener-water solution was added to the mixture gradually and then stirred and sonicated for 10 min. Finally, the steel substrate was dipped into the finally prepared mixture for only 1 min. To facilitate the initial curing, the coated coupons were placed in the oven at 40°C for 24 hours. Thereafter, the coated coupons were cured at ambient temperature and humidity (approximately 21°C and 50% relative humidity) for another 6 days, and a uniform coating was formed and ready for the corrosion testing and surface analysis.

**Table 2.** The average thickness and roughness of 3 samples (#10, #25 and #32) with the best performance for anti-corrosion, vs. the control sample (#33).

| samples     | Average thickness ( $\mu\text{m}$ ) | Average roughness ( $\mu\text{m}$ ) |
|-------------|-------------------------------------|-------------------------------------|
| #10         | 17.00                               | 0.740                               |
| #25         | 13.25                               | 0.108                               |
| #32         | 12.83                               | 0.056                               |
| #33/control | 12.20                               | 0.067                               |

After the morphological investigation and electrochemical test shown in the following sections, the average thickness of 3 nanocomposite coatings (#10, #25 and #32) with the best performance for anti-corrosion and the control sample (#33) were tested using a handheld tester (Digital multi-meters TY700, Yokogawa Corporation of America, Newnan, Georgia). The surface micro-roughness ( $R_a$ ) of each of these four coatings was tested by use of a hand-held roughness tester (Model TR200, Time Group Inc., Beijing, China) with cut-off length of 0.25 mm to 2.5 mm. The portable tester was used to measure at minimum three  $0.8 \times 5 \text{ mm}^2$  areas, from which an average  $R_a$  value was calculated. The coatings' thickness and roughness data are shown in Table 2.

### 2.3. Morphological investigation of coatings

A Field Emission Scanning Electron Microscope (FESEM, Zeiss Supra 55 VP) was used to investigate the surface morphology of the plain epoxy coating and nanocomposite-epoxy coatings. The coatings were removed from the steel coupon's surface, and then sputter-coated with a thin Iridium layer (1 to 2 nm) to avoid the charging effect caused by the non-conductive property of epoxy.

Nanoclays have been extensively utilized to improve the mechanical properties, heat resistance and increased biodegradability of hybrid materials [34]. The non-modified montmorillonite (Nano-clay), which has a plate structure, is a 2-to-1 layered smectite clay mineral, and has abundance of sodium ions and high expansion pressure. The unique structure and its hydrophilicity can lead to exfoliation and dispersion of crystal in the form of micro-particles or layer [35] (see Figure 2). Polymer modified nanoclays can be used as a polymeric photosensitizer [36]. The Polysiloxane-modified montmorillonite (PS-clay) produced from the hydrophilic nanoclay with the organic cation exchange can reduce the permeability of composite material and improves its compression strength [37]. The microstructures of these two types of nanoclays are shown in Figure 2. Note that the PS-clay and Nano-clay feature a bulk density of is  $0.251 \text{ g/cm}^3$  and  $0.678 \text{ g/cm}^3$  respectively and both feature a maximum size of 200–400 nm in terms of aspect ratio [32, 38].

### 2.4. Electrochemical measurements

All the electrochemical tests were conducted by use of a Gamry Potentiostat with a model Reference 600 with a traditional three-electrode system: a platinum mesh serves as counter electrode, a saturated calomel electrode (SCE) servers as reference electrode and the epoxy-coated steel coupon is used as working electrode. The coatings evaluated in the electrochemical measurements had similar thickness as those used in the morphological study since they were prepared following the same procedures. Two methods were used to test the anti-corrosive performance of these nanocomposite coatings in 3.0 wt.% NaCl aqueous solution: electrochemical impedance spectroscopy (EIS). The coating formulations were designed based on a Uniform Design table adopted from <http://www.math.hkbu.edu.hk/UniformDesign>, as shown in Table 1. The coated steel coupons were immersed into the NaCl solution and then periodically tested over 14 days. [39] For EIS measurements, the coupons were periodically polarized at  $\pm 10 \text{ mV}$  around its open circuit potential (OCP) by an alternating current (AC) signal with its frequency ranging from 10 kHz to 10 mHz (10 points per decade) in order to measure their corrosion behavior at the given time of immersion. This provided the data for deriving various parameters related to the coating/electrolyte interface and the steel/electrolyte interface.

### 2.5. Microhardness and DSC measurements

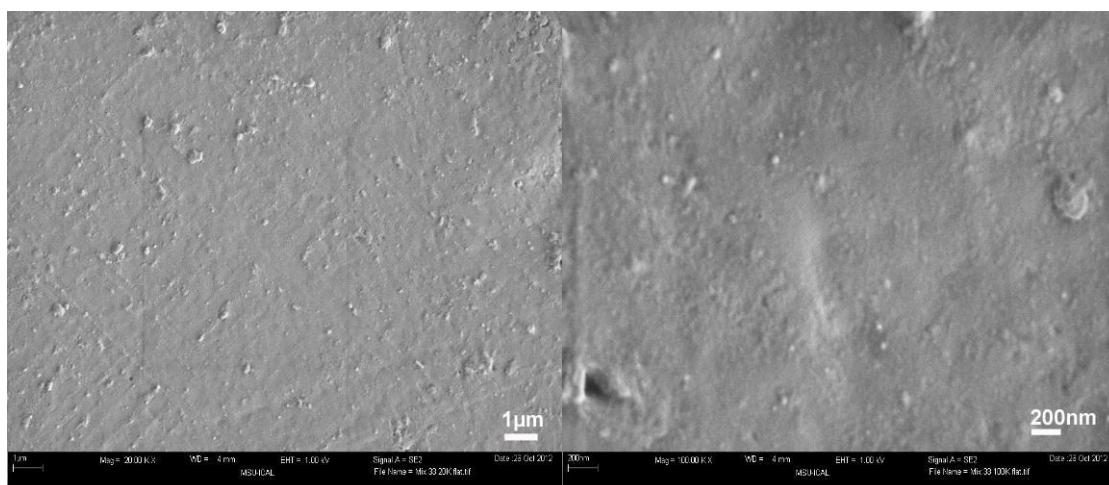
The micro-hardness (Vickers hardness), which can reflect the mechanical properties of epoxy coatings, were measured using a LECO LM Series (LM-700) micro-hardness tester with the following procedures. First, the specimen was flattened on one side using a sander and then placed on the tester.

Then, a digital microscope was used to clearly focus on the epoxy coating and to identify a spot on the surface that did not contain air bubbles. Thereafter, the start button was hit and the machine automatically applied a load using an indenter. Once the correct load was found, a new spot was chosen for testing and the machine was run again. After the indent was made, with the help of the microscope, the length of the indent was measured using two hash marks adjusted in the microscope first horizontally then vertically.

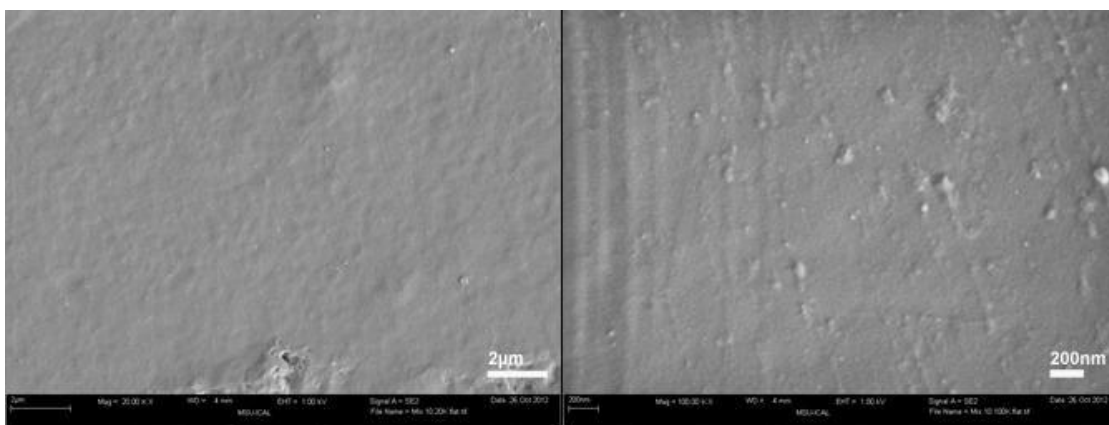
DSC experiments were conducted under argon atmosphere (50 cm<sup>3</sup>/min) using a DSC-Q200 calorimeter (TA Instruments, USA). The samples were heated from 20 to 250 °C at three different heating rates (2 °C, 5 °C and 10 °C), respectively.

### 3. RESULTS AND DISCUSSION

#### 3.1. Effect of nanomaterials on the morphology of epoxy coating



(a)



(b)

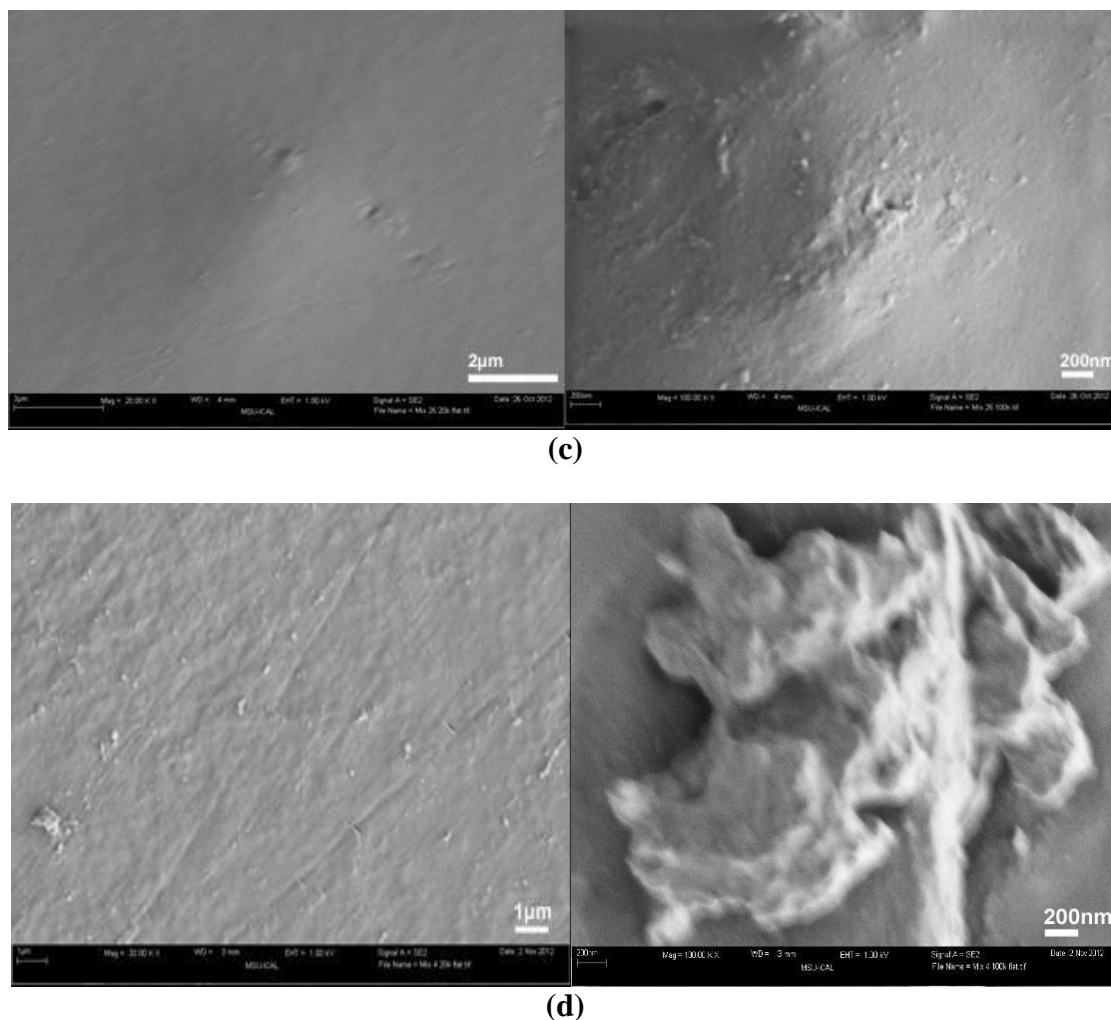


**Figure 3.** FE-SEM micrographs of #33 (a), #10 (b), #25(c) and #32(d) with different magnification (left: representative microstructure at 20K; right: rare defects, at 100K)

The morphologies of the control epoxy coating (#33, plain epoxy without nanomaterials) and the three select nanocomposite coatings are shown in Figure 3. Figure 3a reveals that the cured plain epoxy coating has a relatively homogeneous morphology at both low magnification (20,000 times) and high magnification (100,000 times). At the sub-micron scale, the coating matrix exhibited some defects in the form of clump or pinhole. When nanomaterials were added into the epoxy coating, pinholes were no longer observed in the coating and a generally more homogeneous coating matrix was observed, as illustrated by Figures 3b-3d. This is consistent with previous studies, which found that nanomaterials can prevent epoxy disaggregation during curing, resulting in a more homogenous coating [40].

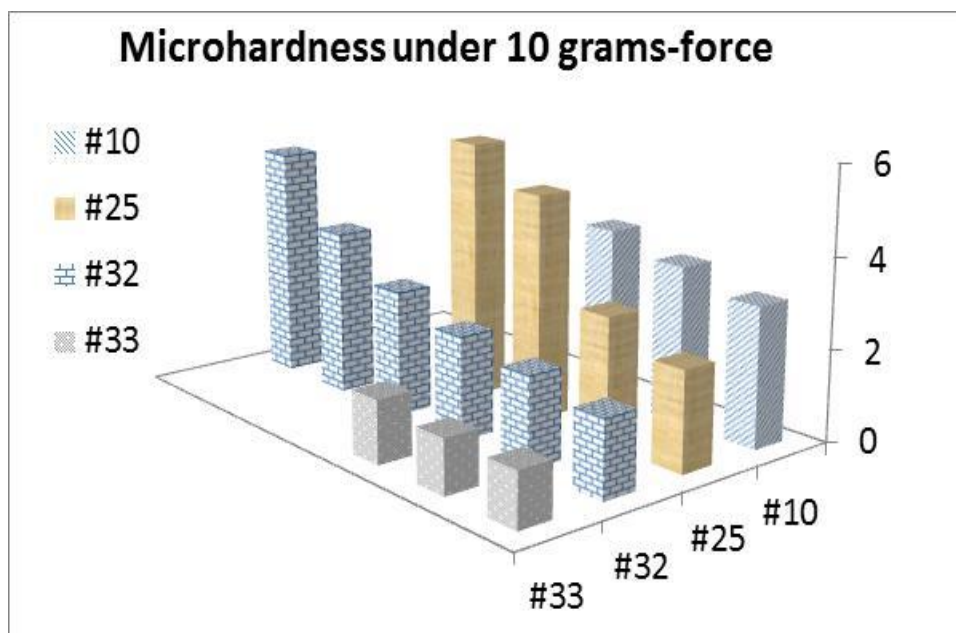
While the vast majority of nanomaterials were apparently well-dispersed into the coating matrix, there were still occasionally sub-micron and micron level agglomeration of nanomaterials, as highlighted in the high-magnification micrographs of Figures 3b-3d. As discussed later, these nanocomposite coatings were selected based on their outstanding anti-corrosion properties. One may hypothesize that better dispersion of the nanomaterials in the coating matrix would further enhance

their anti-corrosion and possibly mechanical properties, as the amount of coating defects (mostly clumps of nanomaterials) would be minimized.

To shed more light on the dispersion of nanomaterials in the coatings, Table 2 presents the thickness and roughness data of the select nanocomposite coatings and the plain epoxy coating. The plain epoxy coating featured an average thickness of 12.20 microns and an average roughness of 0.067 microns. The nano-modification significantly increased the thickness of the cured epoxy coating, with the thickness ranging from 12.83 to 17.0 microns. This is attributable to the increased viscosity in the nanocomposite coatings, as all of them went through the 1-min dip coating step. The effect of nano-modification on the roughness of the cured epoxy coating varied, with the roughness ranging from 0.056 to 0.74 microns. The substantial increase in the coating’s sub-micron roughness is likely the result of nanomaterials agglomeration. Among the three select nanocomposite coatings, the coating formulation #32 exhibited the lowest thickness and roughness values, which coincide with its best anti-corrosion properties among the three (Table 4, as discussed later).

### 3.2. Effect of nanomaterials on the mechanical property of epoxy coating

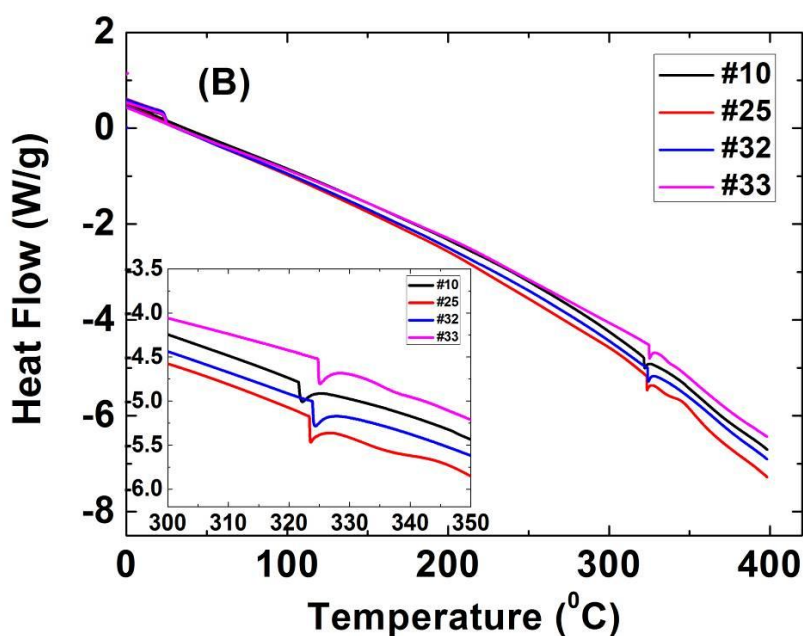
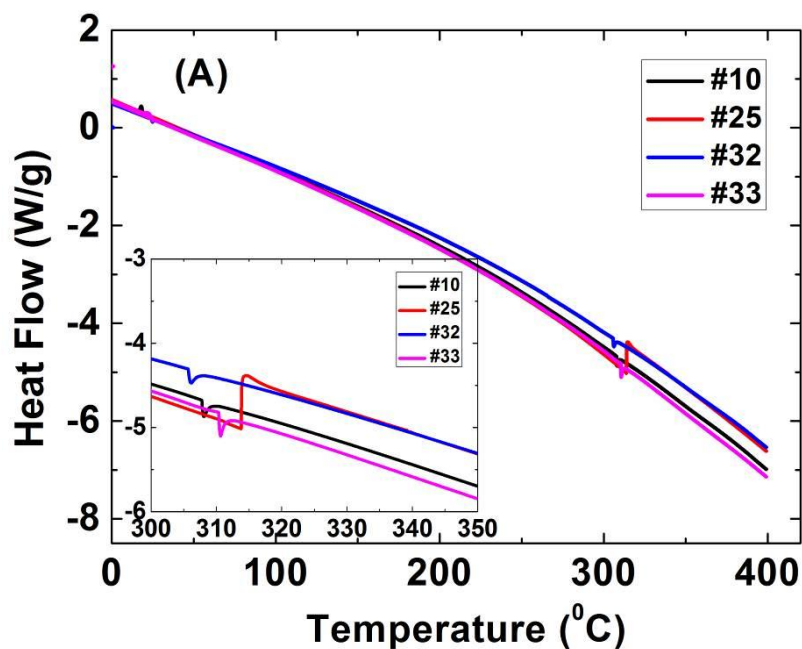
The results of microhardness test from plain epoxy coating and the three select nanocomposite coatings are shown in Figure 4. Regardless of the changes in the coating’s thickness and roughness (shown in Table 2), the microhardness of the three nanocomposite coatings was greatly enhanced, by an average of 230%, 320% and 380% for #32, #25 and #10, respectively. Such enhancements are desirable as they imply great potential for the nanocomposite coatings to achieve better resistance to abrasion, impact, scratch, and similar mechanical damages.



**Figure 4.** Microhardness test results (under 10 grams-force) from control sample (#33, plain epoxy coating) and select nanocomposite coatings (#32, #25, and #10).

The mechanic properties of nanocomposite coatings, represented by the micro-hardness values, depend greatly on the integrity and internal properties of the coating surface. Under the mechanical stress, the micro-voids within the agglomerated nanomaterials or within the polymer matrix may become the origin of micro-cracks or facilitate the propagation of micro-cracks [1]. The nanomaterials can fill pinholes and cavities in the coating matrix, reduce its total free volume, and contribute to crack bridging and crack deflection [1].

3.3. Effect of nanomaterials on the thermal property of epoxy coating



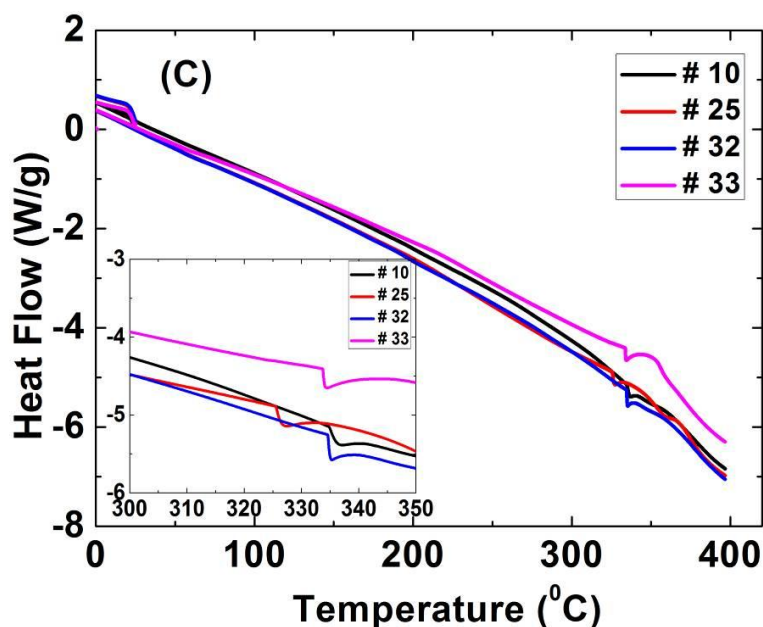


**Figure 5.** DSC thermograms of plain epoxy coating and nanocomposite coatings, with the heating rate of 2 °C/min (A), 5 °C/min (B) and 10 °C/min (C), respectively.

The thermal property of epoxy coatings can be assessed from their DSC thermograms shown in Figure 5. From the DSC data, the glass transition temperatures ( $T_g$ ) of the plain epoxy coating and the three select nanocomposite coatings were derived and presented in Table 3.

**Table 3.** Glass transition temperature ( $T_g$ ) of the control epoxy coating and the nanocomposite epoxy coatings, as a function of heating rate in measuring the DSC thermogram.

| Samples | $T_g$                  |                        |                         |
|---------|------------------------|------------------------|-------------------------|
|         | Heating rate (2°C/min) | Heating rate (5°C/min) | Heating rate (10°C/min) |
| #10     | 308.0                  | 322.6                  | 336.9                   |
| #25     | 306.1                  | 323.7                  | 327.3                   |
| #32     | 313.6                  | 324.5                  | 335.5                   |
| #33     | 310.6                  | 325.0                  | 334.6                   |

It can be observed that the  $T_g$  value of all four coatings increased with the increase in the heating rate during the DSC measurement, which is in accordance with previous reports [41-43]. It has been reported that the  $T_g$  may increase [6, 44-46], decrease [33, 47-49], not change [50, 51], or even show non-monotonic trend [52-54] as a function of filler content. In general, the nano-modification in

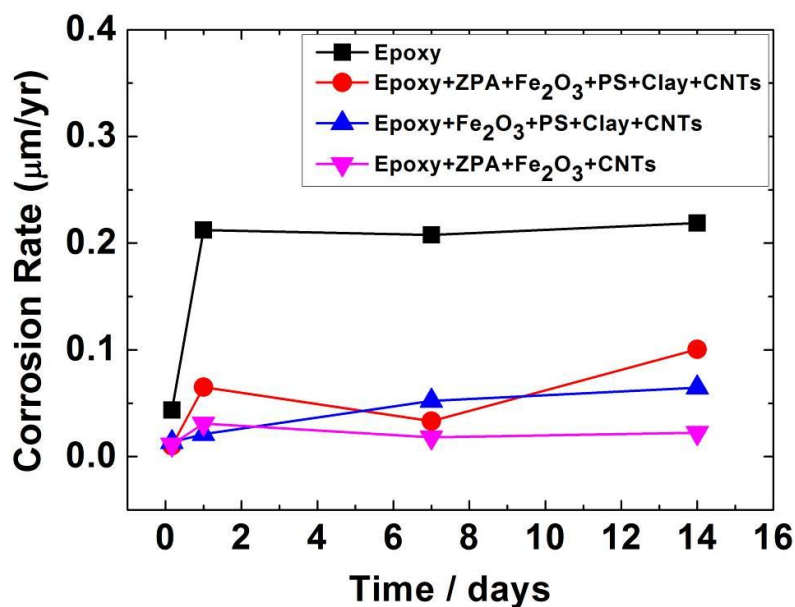
this work slightly decreased the  $T_g$  of the epoxy coating at 2°C/min and 5°C/min and slightly increased it at 10°C/min, implying the complicated interactions between the external heating and the thermal behavior of the nanocomposite coatings. Note that an increase in the  $T_g$  may reduce chain segmental motions and improve stiffness [1, 43].

### 3.4. Effect of nanomaterials on the anti-corrosion properties of coated steel

EIS measurements were taken to investigate the anti-corrosion properties of the select waterborne epoxy coatings on the steel substrate. The corrosion potential, polarization resistance, instantaneous corrosion rate and other electrochemical parameters were estimated from these electrochemical measurements.

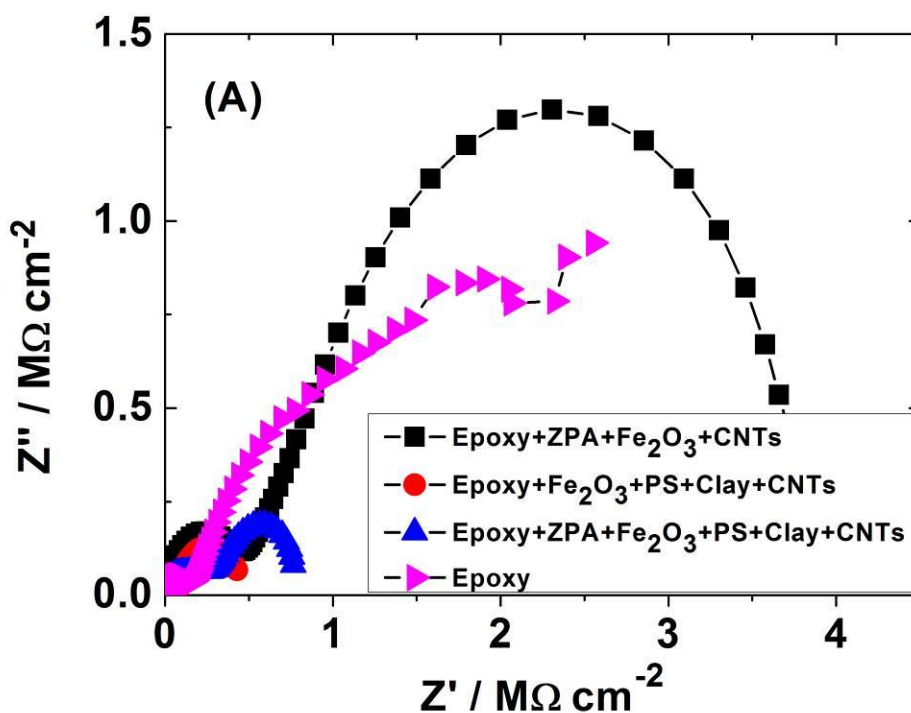
Figure 6 illustrates the temporal evolution of instantaneous corrosion rate of the steel coated by various waterborne epoxy coatings listed in Table 1 during a 14-day immersion in 3.0 wt.% NaCl solution, based on the weak polarization measurements. It could be seen that the incorporation of small amounts of nanomaterials and inorganic corrosion inhibitor (no more than 3.25% and 1.5% by total weight of epoxy coating, respectively) into the epoxy coating would reduce the corrosion rate of the epoxy-coated steel in the aggressive electrolyte greatly. In other words, such modification could greatly enhanced the polarization resistance of the epoxy-coated steel in the electrolyte, from approximately 30 KOhm.cm<sup>-2</sup> up to approximately 110 KOhm.cm<sup>-2</sup> at day 14. Of all the 32 nanocomposite coatings listed in Table 1, #10, #25 and # 32 exhibited the best anti-corrosion performance (i.e., lowest corrosion rate of steel) in 3.0 wt.% NaCl solution after 14 days of immersion. For these three “best performers”, the nanomaterials incorporated into the waterborne epoxy coating were able to reduce the corrosion rate of the steel substrate by up to 5 times over the 14-day immersion period. In our previous work [1], the nano-modification of a solvent-based epoxy coating reduced the corrosion rate of the carbon steel much more considerably than that reported for this waterborne epoxy coating. One main reason is that in 3% NaCl solution, the control waterborne epoxy coating featured much better corrosion resistance (~0.2 μm/yr corrosion rate of steel) than the control solvent-based epoxy coating (~10 μm/yr corrosion rate of steel).

In other words, the benefits of nano-modification are coating specific and they diminished when the neat epoxy coating already had dense microstructure and barrier properties. Arguably, another factor to consider is that certain nano-modification (e.g., by carbon nanotubes) greatly reduced the electrical resistance of the epoxy coating and thus the measured  $R_p$ , thus leading to an overestimate of actual corrosion rate of the steel substrate. As we reported previously [1], the measured  $R_p$  consisted of a component characteristic of the coating-electrolyte interface inside the coating and another component characteristic of the steel-electrolyte interface. For non-conductive coatings, the  $R_p$  can be used to estimate corrosion resistance of the steel at the steel-electrolyte interface and can be used to evaluate the anti-corrosion properties of the coatings. For coatings with conductive nanotubes incorporated, however, it may be more reasonable to use the charge transfer resistance to estimate the corrosion rate of the steel under the coating.



**Figure 6.** Dependence of the corrosion rate of epoxy-coated steel on time in 3.0 wt.% NaCl solution for different nanomaterial

Figure 7 presents the Nyquist diagrams of the steel coated by the select waterborne epoxy coating after a 14-day immersion in 3.0 wt.% NaCl solution. The Nyquist diagrams derived from the EIS measurements featured two capacitive loops, with the high-frequency loop (A) and the low-frequency loop (B) attributed to the resistance and capacitance of the coating-electrolyte and of the steel-electrolyte interfaces, respectively.



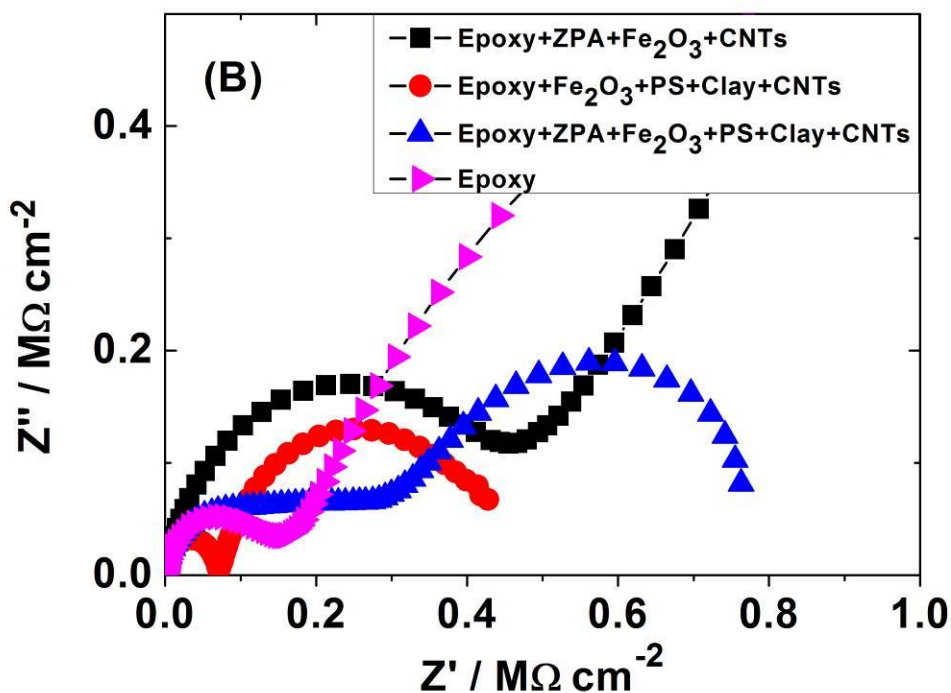


**Figure 7.** EIS Nyquist diagrams for epoxy-coated steel after 14 days in 3.0 wt. % NaCl solution. Their impedance data were plotted at full scale (A) and low scale (B).

The complex impedance of the surface-electrolyte interfaces depends on the frequency of the externally imposed alternating current polarization signal, which allows the representation of the system with an equivalent circuit typically consisting of resistors and capacitors.

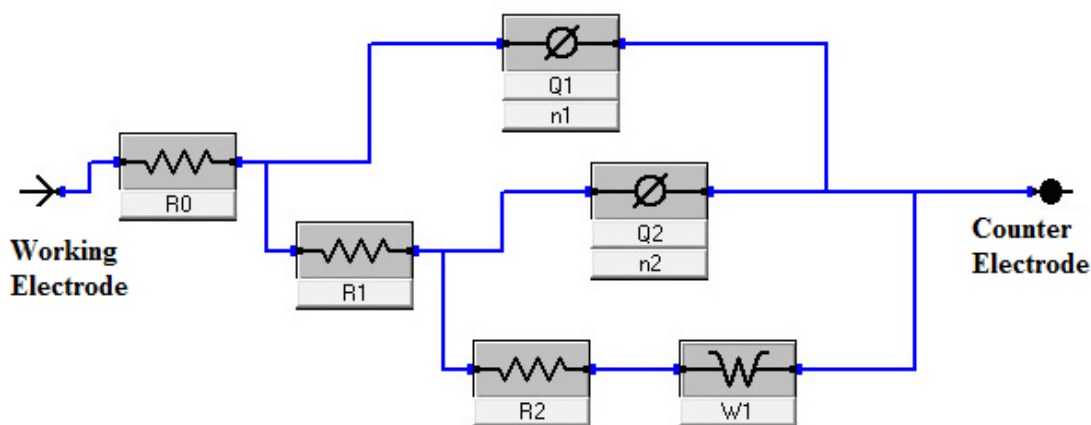


**Figure 8.** Equivalent electric circuit used for fitting the electrochemical impedance spectra.

For this study, the equivalent circuit shown in Figure 8 was applied to evaluate the level of corrosion protection through the test from the select nanocomposite coatings. Constant phase elements ( $Q$ ) instead of capacitances were used in all fittings. Such modification is obligatory when the phase angle of capacitor is different from  $-90^\circ$ . The obtained parameters are given in Table 4, where  $R_1$  and

$Q_1$  are the resistance and capacitance of coating characteristic of its pore network structure (the coating-electrolyte interface inside the coating), and  $R_2$  and  $Q_2$  are the charge transfer resistance of the steel (coupon) and the double layer capacitance on the steel surface (the steel-electrolyte interface), respectively.  $R_0$  is the solution resistance between the counter electrode and the working electrode (coated steel), which depends on the resistivity of electrolyte (ionic concentration, type of ions, temperature, etc.) and the geometry of the area in which current is carried.  $R_0$  is not related to the property of coating layers and is thus not discussed in this case, whereas  $n_1$  and  $n_2$  are the fitting coefficient for  $Q_1$  and  $Q_2$ , respectively, in which the number “1” is the perfect fit of a capacitor and the number “0” is the worst fit.

**Table 4.** Parameters of the equivalent electric circuits, derived from the EIS data from the coated steels after 14 days in 3.0 wt.% NaCl solution.

| Coating product  | $R_1$ ( $\Omega \cdot \text{cm}^2$ ) | $R_2$ ( $\Omega \cdot \text{cm}^2$ ) | $Q_1$ ( $\text{F} \cdot \text{cm}^{-2}$ ) | $Q_2$ ( $\text{F} \cdot \text{cm}^{-2}$ ) | $W_1$ ( $\text{mS cm}^{-2}$ ) | OCP (V) |
|--|--------------------------------------|--------------------------------------|---|---|-------------------------------|---------|
| Plain epoxy  | 1.28E + 04                           | 4.48E + 04                           | 5.05E - 06                                | 5.22E - 06                                | 8.87E - 5                     | -0.681  |
| Epoxy+ZPA+Fe <sub>2</sub> O <sub>3</sub> +PS+Clay+CNTs | 2.78E + 05                           | 2.81E + 07                           | 9.22E - 10                                | 1.92E - 08                                | 4.70E - 6                     | -0.602  |
| Epoxy+Fe <sub>2</sub> O <sub>3</sub> +PS+Clay+CNTs     | 1.35E + 05                           | 1.78E + 07                           | 9.74E - 10                                | 3.34E - 07                                | 1.46E - 7                     | -0.532  |
| Epoxy+ZPA+Fe <sub>2</sub> O <sub>3</sub> +CNTs         | 2.36E + 06                           | 5.14E + 07                           | 8.43E - 10                                | 1.79E - 09                                | 9.41E - 9                     | -0.656  |

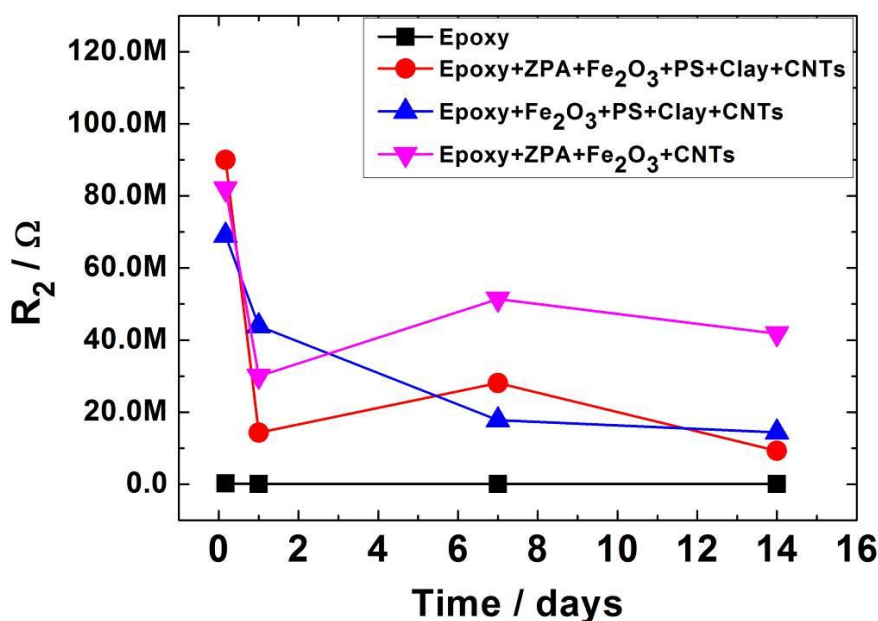


**Figure 9.** Charge transfer resistance ( $R_2$ ) for coated carbon steel coupons in 3.0 wt.% NaCl solution.

From Table 4, it is evident that the select nanocomposite coatings (#10, #25 and #32) can greatly reduce coating porosity and improve barrier performance for corrosion protection of the steel substrate, with their coating resistance  $R_1$  increased by 11-185 times and “capacitance”  $Q_1$  decreased by 348-599 times related to the plain epoxy coating (#33). These nanocomposite coatings also significantly increased the charge transfer resistance  $R_2$  by 397 ~ 1147 times and reduced the double layer capacitance  $Q_2$  by 6~ 343 times, indicating that the coatings could greatly enhance corrosion resistance of the steel at the steel-electrolyte interface.

Figure 9 shows the evolution of the charge transfer resistance ( $R_2$ ) over the time of 14-day continuous immersion in 3.0 wt.% NaCl, which confirms the outstanding anti-corrosion benefits provided by the modifiers to the epoxy coated steel. Table 4 also suggests that the incorporation of nanomaterials and/or inorganic corrosion inhibitor induced a noble shift to the open circuit potential (OCP) of the coated steel and considerably reduced the Warburg impedance ( $W_1$ ) indicative of the diffusion resistance of molecules within the double layer. Our result is compared to other works, which are listed in Table 5 [55-58]. From Table 5, it can be seen that the value of coating resistance  $R_1$  and the charge transfer resistance  $R_2$  obtained by this coating product (Epoxy+ZPA+Fe<sub>2</sub>O<sub>3</sub>+CNTs) is higher than most of the others, indicating that nanomaterials-based composites have excellent anti-corrosion properties for the protection of metal components.

**Table 5.** Comparison of the Corrosion Inhibitors for Steel Substrates\*

| No. | Corrosion inhibitors   | $R_1$ ( $\Omega \cdot cm^2$ ) | $R_2$ ( $\Omega \cdot cm^2$ ) | Ref.      |
|-----|--|-------------------------------|-------------------------------|-----------|
| 1   | Epoxy+E-SiO <sub>2</sub> +GPTMS  | 5.43E+05                      | 6.22E+05                      | [55]      |
| 2   | Alkyd+Li <sub>0.5</sub> Mn <sub>0.25</sub> Ti <sub>2</sub> (PO <sub>4</sub> ) <sub>3</sub> | 3.47E+06                      | 1.55E+07                      | [56]      |
| 3   | Epoxy+MET+GME  | 1.5E+05                       | 2.0E+05                       | [57]      |
| 4   | Epoxy+ $\beta$ -cyclodextrin+MWCNTs+<br>benzimidazole                                      | 2.36E+05                      | 2.34E+05                      | [58]      |
| 5   | Epoxy+F-AgNPs/DGEBA  | —                             | 1.27E+08                      | [59]      |
| 6   | Epoxy+ZPA+Fe <sub>2</sub> O <sub>3</sub> +CNTs   | 2.36E + 06                    | 5.14E + 07                    | This work |

\* Abbreviation: E-SiO<sub>2</sub>(electrodeposited SiO<sub>2</sub>), GPTMS((3-glycidoxypropyl)-trimethoxysilane), MWCNTs(multi-walled carbon nanotubes), MET(metronidazole), GME(graphene oxide composite).

#### 4. CONCLUSIONS

The main findings of this exploratory research are provided as follows.

- The benefits of nano-modification are coating specific and there are synergistic effects between the different types of nano-materials admixed into the waterborne epoxy coating.
- The co-incorporation of small amount of multi-wall carbon nanotube with other nanomaterials into the waterborne epoxy coating led to significant improvements in its anti-corrosion performance on the steel substrate and the microhardness of the coating.

- The incorporation of small amount of ZPA or nano-Fe<sub>2</sub>O<sub>3</sub> into the waterborne epoxy coating led to outstanding corrosion resistance. In contrast, the admixing of non-modified montmorillonite did not greatly improve the corrosion resistance of the waterborne epoxy coating, as the hydrophilic nanoclay mostly served to improve the barrier properties of the coating. The admixing of polymer-modified montmorillonite into the waterborne epoxy coating did not greatly improve its corrosion resistance, likely due to the difficulty of fully dispersing such hydrophobic nanoclay in the aqueous system.

- At least two possible mechanisms have been provided to explain the enhanced corrosion protection of nanocomposite epoxy coating. The nanomaterials used in this study could improve the quality of the cured epoxy coating, reduce the porosity of the coating matrix, and zigzag the diffusion path available by deleterious species, which lead to the improvement of barrier performance of the epoxy coating. Meanwhile, nanomaterials altered the physicochemical properties of the coating-steel interface.

For future research, it would be important to explore surface functionalization of carbon nanotubes [60] and better dispersion of the nanomaterials in the epoxy matrix so as to maximize the benefits of such nano-modification of epoxy coating. To enable long-term anti-corrosion performance of the nanocomposite coatings, one should also investigate the application of multiple nanomaterials as reservoirs for the storage and prolonged lease of corrosion inhibitors [61-64] or the combined use of nano-modification and self-healing technologies [18].

#### ACKNOWLEDGEMENTS

XX and YL gratefully acknowledge financial support from the National Science Foundation of China (No. 20975002); The authors gratefully acknowledge financial support by the ChuTian Scholar Visiting Professorship Fund provided by the Hubei Department of Education, China, as well as financial support by the U.S. DOT Research and Innovative Technology Administration (WTI UTC) and the National Science Foundation of China (No. 51278390, WPU).

#### References

1. X. M. Shi, T. A. Nguyen, Z. Y. Suo, Y. J. Liu, and R. Avci, *Surface & Coatings Technology*, 204(2009) 237.
2. F. Galliano and D. Landolt, *Progress in Organic Coatings*, 44(2002) 217.
3. V. B. Miskovic-Stankovic, M. R. Stanic, and D. M. Drazic, *Progress in Organic Coatings*, 36(1999) 53.
4. A. Talo, O. Forsen, and S. Ylasaari, *Synthetic Metals*, 102(1999) 1394.
5. S. Jones, N. Martys, Y. Lu, and D. Bentz, *Cement and Concrete Composites*, 58(2015) 59.
6. B. Wetzal, F. Hauptert, and M. Q. Zhang, *Composites Science and Technology*, 63(2003) 2055.
7. A. C. Loos and G. S. Springer, *Journal of Composite Materials*, 13(1979) 131.
8. S. Yamini and R. J. Young, *Polymer*, 18(1977) 1075.
9. D. Perreux and C. Suri, *Composites Science and Technology*, 57(1997) 1403.
10. F. Tang, G. Chen, and R. K. Brow, *Cement and Concrete Research*, 82(2016) 58.
11. V. Cannillo, F. Bondioli, L. Lusvardi, M. Montorsi, M. Avella, M. E. Errico, and M. Mahnconco, *Composites Science and Technology*, 66(2006) 1030.
12. M.-C. Chen, Y. Chang, C.-T. Liu, W.-Y. Lai, S.-F. Peng, Y.-W. Hung, H.-W. Tsai, and H.-W. Sung, *Biomaterials*, 30(2009) 79.

13. J. M. Hu, J. Q. Zhang, and C. N. Cao, *Progress in Organic Coatings*, 46(2003) 273.
14. M. Behzadnasab, S. M. Mirabedini, K. Kabiri, and S. Jamali, *Corrosion Science*, 53(2011) 89.
15. I. E. dell'Erba, C. E. Hoppe, and R. J. J. Williams, *Langmuir*, 26(2010) 2042.
16. L. T. Keene, M. J. Vasquez, C. R. Clayton, and G. P. Halada, *Progress in Organic Coatings*, 52(2005) 187.
17. E. Langer, H. Kuczynska, E. Kaminska-Tarnawska, and J. Lukaszczyk, *Progress in Organic Coatings*, 71(2011) 162.
18. A. Madhankumar, S. Nagarajan, N. Rajendran, and T. Nishimura, *Journal of Solid State Electrochemistry*, 16(2012) 2085.
19. B. Ramezanzadeh and M. M. Attar, *Materials Chemistry and Physics*, 130(2011) 1208.
20. M. Sangermano, I. Roppolo, G. Shan, and M. P. Andrews, *Progress in Organic Coatings*, 65(2009) 431.
21. X. Shi, T. A. Nguyen, Z. Suo, Y. Liu, and R. Avci, *Surface & Coatings Technology*, 204(2009) 237.
22. G. Kortaberria, P. Arruti, A. Jimeno, I. Mondragon, and M. Sangermano, *Journal of Applied Polymer Science*, 109(2008) 3224.
23. M. Sangermano, G. Malucelli, E. Amerio, A. Priola, E. Billi, and G. Rizza, *Progress in Organic Coatings*, 54(2005) 134.
24. M. Sangermano, A. Priola, G. Kortaberria, A. Jimeno, I. Garcia, I. Mondragon, and G. Rizza, *Macromolecular Materials and Engineering*, 292(2007) 956.
25. Y. Tang, L. Ye, S. Deng, C. Yang, and W. Yuan, *Materials & Design*, 42(2012) 471.
26. O. Zabihi, A. Hooshafza, F. Moztarzadeh, H. Payravand, A. Afshar, and R. Alizadeh, *Thermochimica Acta*, 527(2012) 190.
27. W.-B. Xu, S.-P. Bao, and P.-S. He, *Journal of Applied Polymer Science*, 84(2002) 842.
28. G. Khanbabaei, J. Aalaie, A. Rahmatpour, A. Khoshniyat, and M. A. Gharabadian, *Journal of Macromolecular Science Part B-Physics*, 46(2007) 975.
29. L. Wang, K. Wang, L. Chen, Y. Zhang, and C. He, *Composites Part A: Applied Science and Manufacturing*, 37(2006) 1890.
30. L. H. Yang, F. C. Liu, and E. H. Han, *Progress in Organic Coatings*, 53(2005) 91.
31. N. Wang, K. Cheng, H. Wu, C. Wang, Q. Wang, and F. Wang, *Progress in Organic Coatings*, 75(2012) 386.
32. X. He and X. Shi, *Transportation Research Record*, (2008) 13.
33. Y. Y. Sun, Z. Q. Zhang, K. S. Moon, and C. P. Wong, *Journal of Polymer Science Part B-Polymer Physics*, 42(2004) 3849.
34. S. W. Goh, M. Akin, Z. You, and X. Shi, *Construction and Building Materials*, 25(2011) 195.
35. S. G. Jahromi and A. Khodaii, *Construction and Building Materials*, 23(2009) 2894.
36. D. Drozd, K. Szczubialka, and M. Nowakowska, *Journal of Photochemistry and Photobiology A: Chemistry*, 215(2010) 223.
37. M. W. Simon, K. T. Stafford, and D. L. Ou, *Journal of Inorganic and Organometallic Polymers and Materials*, 18(2008) 364.
38. Z. Yang, X. Shi, A. T. Creighton, and M. M. Peterson, *Construction and Building Materials*, 23(2009) 2283.
39. Y. Li, P. Kumar, X. Shi, T. A. Nguyen, Z. Xiao, and J. Wu, *Int. J. Electrochem. Sci.*, 7(2012) 8151.
40. F. Dietsche, Y. Thomann, R. Thomann, and R. Mulhaupt, *Journal of Applied Polymer Science*, 75(2000) 396.
41. D. Souri, *Measurement*, 44(2011) 2049.
42. I. Avramov, G. Guinev, and A. C. M. Rodrigues, *Journal of Non-Crystalline Solids*, 271(2000) 12.
43. S. Vyazovkin, N. Sbirrazzuoli, and I. Dranca, *Macromolecular Rapid Communications*, 25(2004) 1708.
44. B. Wetzels, P. Rosso, F. Haupt, and K. Friedrich, *Engineering Fracture Mechanics*, 73(2006) 2375.

45. J. Ma, M.-S. Mo, X.-S. Du, P. Rosso, K. Friedrich, and H.-C. Kuan, *Polymer*, 49(2008) 3510.
46. S. Kang, S. I. Hong, C. R. Choe, M. Park, S. Rim, and J. Kim, *Polymer*, 42(2001) 879.
47. H. Miyagawa, M. J. Rich, and L. T. Drzal, *Thermochimica Acta*, 442(2006) 67.
48. B. J. Ash, L. S. Schadler, and R. W. Siegel, *Materials Letters*, 55(2002) 83.
49. G. Liu, H. Zhang, D. J. Zhang, Z. Zhang, X. F. An, and X. S. Yi, *Journal of Materials Science*, 47(2012) 6891.
50. P. Rosso and L. Ye, *Macromolecular Rapid Communications*, 28(2007) 121.
51. J. T. Han and K. Cho, *Journal of Materials Science*, 41(2006) 4239.
52. G. Zhang, Z. Rasheva, J. Karger-Kocsis, and T. Burkhart, *Express Polymer Letters*, 5(2011) 859.
53. M. Preghenella, A. Pegoretti, and C. Migliaresi, *Polymer*, 46(2005) 12065.
54. S. Barrau, P. Demont, C. Maraval, A. Bernes, and C. Lacabanne, *Macromolecular Rapid Communications*, 26(2005) 390.
55. Y.-H. Liu, X.-H. Jin, and J.-M. Hu, *Corrosion Science*, 106(2016) 127.
56. M. A. Deyab, K. Eddahaoui, R. Essehli, S. Benmokhtar, T. Rhadfi, A. De Riccardis, and G. Mele, *Journal of Molecular Liquids*, 216(2016) 699.
57. Z. Yu, L. Lv, Y. Ma, H. Di, and Y. He, *RSC Advances*, 6(2016) 18217.
58. Y. He, C. Zhang, F. Wu, and Z. Xu, *Synthetic Metals*, 212(2016) 186.
59. R. Manjumeena, R. Venkatesan, D. Duraibabu, J. Sudha, N. Rajendran, and P. T. Kalaichelvan, *Silicon*, 8(2016) 277.
60. H.-J. Song, Z.-Z. Zhang, and X.-H. Men, *European Polymer Journal*, 43(2007) 4096.
61. D. G. Shchukin and H. Möhwald, *Advanced Functional Materials*, 17(2007) 1451.
62. D. Fix, D. V. Andreeva, Y. M. Lvov, D. G. Shchukin, and H. Möhwald, *Advanced Functional Materials*, 19(2009) 1720.
63. Y. M. Lvov, D. G. Shchukin, H. Mohwald, and R. R. Price, *Acs Nano*, 2(2008) 814.
64. E. Abdullayev and Y. Lvov, *Journal of Nanoscience and Nanotechnology*, 11(2011) 10007.